Journal of Chromatography A 1781 (2026) 467072

Contents lists available at ScienceDirect

Journal of Chromatography A

journal homepage: www.elsevier.com/locate/chroma

Investigation of adsorption behavior and scale up for hydroxysafflor yellow A purification from Safflower: a case study

Amin Tabesh [a], Hassan Rezadoost [a,*], Masoud Rahimi [a,b], Hamid Reza Norouzi [c], Simona Felletti [d,*], Alberto Cavazzini [e,f]

[a] Department of Phytochemistry, Medicinal Plants and Drugs Research Institute, Shahid Beheshti University, Evin, Tehran 1983963113, Iran
[b] Department of Pharmaceutical Engineering, Medicinal Plants and Drugs Research Institute, Shahid Beheshti University, Tehran 1983969411, Iran
[c] Center of Engineering and Multiscale Modeling of Fluid Flow (CEMF), Department of Chemical Engineering, Amirkabir University of Technology (Tehran Polytechnic), Tehran, Iran
[d] Department of Environmental and Prevention Sciences, University of Ferrara, via L. Borsari 46, Ferrara 44121, Italy
[e] Department of Chemical, Pharmaceutical and Agricultural Sciences, University of Ferrara, via L. Borsari 46 44121, Ferrara, Italy
[f] Council for Agricultural Research and Economics, CREA, via della Navicella 2/4, Rome, Italy

ARTICLE INFO

Keywords:
Enrichment
Hydroxysafflor yellow A
Isotherm parameters
Mathematical modeling
Preparative chromatography

ABSTRACT

Given the complexity of natural extracts, multiple purification steps are often required to satisfy strict purity requirements for the isolated product. In this context, mathematical modeling could be a useful tool to evaluate the feasibility of large-scale purification and to find optimal elution conditions without relying on the traditional trial-and-error method. In this work, the thermodynamic behavior of Hydroxysafflor yellow A (HSYA), the primary bioactive pigment in the safflower plant, has been modeled and simulated under gradient elution conditions in analytical scale to find optimal parameters for its isolation under preparative scale. Adsorption isotherm parameters were determined through the so-called inverse method in the analytical scale and further confirmed in the preparative scale. The general rate model accurately predicted elution profiles by considering all mass transfer resistances between the stationary and mobile phases, with excellent agreement between simulated and experimental data. It resulted that the optimization of process operating variables led to an increase of the HSYA purity from 20% (crude extract) to 80% (after enrichment), and further purified to 95% using reversed-phase preparative chromatography. The proposed workflow offers a scalable and sustainable strategy for purifying a natural compound using enrichment and subsequent purification techniques.

1. Introduction

Safflower (*Carthamus tinctorius* L.), a plant belonging to the *Compositae* (*Asteraceae*) family [1], is a valuable source of natural pigments and bioactive compounds [2]. Generally, two classes of pigments, namely yellow and red pigments, have been identified in this plant. The yellow pigments have been employed as natural colorants in the food and cosmetic industries [3]. The main component of the yellow pigments is identified as Hydroxysafflor yellow A (HSYA), a quinochalcone C-glycoside, which demonstrated remarkable therapeutic potential in cardiovascular diseases, cerebral ischemia, neuroprotection, and antioxidant activity [3–7]. This compound can also be considered as a key reference marker for the quality assessment of safflower related products [8–12]. However, the presence of similar constituents in the crude safflower extract hinders the purification of HSYA. Various conventional approaches have been employed for HSYA isolation from Safflower extracts including macroporous adsorption resins [9,10], high-speed countercurrent chromatography (HSCC) [13], flash chromatography, and preparative reversed-phase chromatography [14]. These methods are generally characterized by moderate purity (typically <90%), low recovery, high solvent usage, and limited scalability. Also, most of the time, the optimum process condition was obtained by trail-and error methods. In this context, mathematical modeling could be helpful in the method development stage for the prediction of elution profiles and the determination of optimal operating conditions applied for large-scale chromatography without relying on time- and resource-consuming trail-and error method [15–18], thereby saving time and sample material [15,19–21]. Despite these advantages, only few examples of the

* Corresponding authors.
E-mail addresses: h_rezadoost@sbu.ac.ir (H. Rezadoost), fllsmn1@unife.it (S. Felletti).

https://doi.org/10.1016/j.chroma.2026.467072
Received 10 March 2026; Received in revised form 16 April 2026; Accepted 6 May 2026
Available online 9 May 2026

application of mathematical models to preparative chromatography are reported. Hooshyari et al [22] employed a mathematical model to purify cannabidiol from a *Cannabis sativa* L. extract reaching 94% of final purity, with an increase in purity of more than 150%; Benedini et al [23] executed a mathematical model for optimizing the purification of proteins in a complex mixture, obtaining +34% of purity; Hossainzadeh et al [24] applied mathematical modeling for the purification of the foot and mouth disease vaccine, reaching a final purity of 85%; Cavazzini et al [25] investigated the retention behavior of a peptide under analytical scale and gradient elution conditions, to name but a few. In this context, the present work is aimed at expanding and demonstrating the applicability of chromatographic modeling to other complex natural matrices, further enhancing the final process performance.

From a practical viewpoint, to implement a more accurate model for the prediction and the optimization of elution profiles, the estimation of the isotherm parameters of the target compound is considered as a determinant step. Different techniques have been utilized for the determination of adsorption isotherm parameters, including: frontal analysis (FA) [26], perturbation method (PM) [27], frontal analysis by characteristic point (FACP) [28], and retention time method (RTM) [29]. Despite their wide application, these methods have several drawbacks, such as requiring relatively large amounts of samples, solvents, and time. An alternative approach is the so-called Inverse Method (IM), which is useful for the more accurate and faster determination of both single-component and competitive isotherms. In this method, the adsorption isotherm is estimated based on minimizing the sum of the least squares between experimental and calculated profiles under the overloading condition [29–33].

In this work, the two-step purification of HSYA from safflower has been modeled and performed firstly using a macroporous resin (enrichment step) and finally using octadecyl silica to reach the desired final purity of 95%. In more detail, the retention behavior, phase equilibria and loading conditions of HSYA have been investigated in the enrichment step under gradient elution conditions. Then the calculated parameters from the analytical scale, by maintaining the type of stationary, linear velocity, and isotherm parameters, were applied to predict the elution profiles in the preparative-scale column.

2. Theory

Mathematical modeling plays a pivotal role in the scale-up and optimization of chromatographic processes, particularly for preparative-scale separations of natural compounds [22]. A robust model can aid in optimizing the operational conditions and predicting the elution profiles on the preparative scale [34]. In this study, the General Rate Model (GRM) was employed to describe the transport and adsorption behavior of HSYA in both analytical and preparative macroporous resin columns under gradient elution conditions. The GRM provides a detailed mechanistic description by accounting for all major mass transfer phenomena as compared with other simplified models, such as the ideal model, equilibrium dispersive model (EDM), transport model, and transport dispersive model, making it particularly suitable for large particle stationary phases such as macroporous resins [35,36]. The following assumptions were incorporated into the model [37]: the chromatographic process is isothermal, the velocity of the mobile phase is constant (its compressibility is negligible), the bed is packed with particles of a porous adsorbent that are spherical and uniform in size, the concentration gradient in the radial direction of the bed is negligible. Local equilibrium exists for the desired component between the pore surface and the stagnant fluid phase in the macropores resin. The dispersion coefficient is constant, and the radial dispersion is negligible. Based on the mentioned assumptions, the mass balance equations in the mobile and the stationary phases for the component i [28,36] are as follows:

$$\frac{\partial c_i}{\partial t}+v\frac{\partial c_i}{\partial z}+\frac{1-\varepsilon}{\varepsilon}\frac{3k_{fi}}{r_p}\left[c_i-c_{pi}\left(r=r_p\right)\right]=D_{ai}\frac{\partial^2 c_i}{\partial z^2} \tag{1}$$

$$\varepsilon_p\frac{\partial c_{pi}}{\partial t}+\left(1-\varepsilon_p\right)\frac{\partial c^*_{pi}}{\partial t}-D_{pi}\varepsilon_p\frac{1}{r^2}\frac{\partial}{\partial r}\left(r^2\frac{\partial c_{pi}}{\partial r}\right)=0 \tag{2}$$

where c_i is the concentration of the component i in the mobile phase, c_{pi} is the concentration of the component i inside the pore particle, c^*_{pi} is the concentration of the component i adsorbed in the stationary phase, ε, and ε_p represent the bed voidage and particle porosity, respectively. D_{pi} is referred to the intra-particle diffusion, which can be calculated by Eq. (3). D_{mi} is the molecular diffusion, which is determined using the Stokes-Einstein Eq. (4) [29].

$$D_{pi}=\frac{\varepsilon_p}{\left(2-\varepsilon_p\right)^2}D_{mi} \tag{3}$$

$$D_{mi}=2.74\times10^{-9}(Mw)^{\frac{-1}{3}} \tag{4}$$

where Mw is the molecular weight of the desired compound.

D_{ai} represents the axial dispersion, which can be calculated based on the equation proposed by Rastegar and Gu [38]:

$$D_{ai}=0.7D_{mi}+\frac{2r_p v\varepsilon}{0.18+0.008(R_e)^{0.59}} \tag{5}$$

where r_p, v, and R_e denote the radius of the particle, linear velocity, and Reynolds number, respectively.

Film mass transfer coefficient for the component i (k_{fi}) is estimated based on the Wilson–Geankoplis correlation [39]:

$$k_{fi}=\frac{1.09}{\varepsilon}\frac{D_{mi}}{d_p}\left(\varepsilon\frac{d_p v}{D_{mi}}\right)^{0.33} \tag{6}$$

2.1. Isotherm model

Estimating the adsorption isotherm is one of the most critical steps in chromatographic modeling. It should be pointed out that the separation efficiency of the target compound improves significantly by variation of organic modifier concentration with time. Therefore, in this study, the adsorption isotherm was estimated under gradient elution conditions. During the gradient elution, the percentage of the organic modifier (φ) gradually increases over the gradient time (t_g). As a result, the amount of adsorption in the stationary phase depends not only on the solute concentration in the mobile phase but also on changes in the organic modifier [25,40].

The Linear Solvent Strength (LSS) model is used to describe the relation between the retention factor (k) and the percentages of an organic modifier [41–43]:

$$\mathrm{Ln}k(\varphi)=-S(\varphi)+\mathrm{Ln}k_0 \tag{7}$$

In this correlation, k_0, the retention factor is extrapolated at $\varphi=0$ and, S is the coefficient characteristic associated with the solute-mobile phase system. To estimate isotherm parameters under gradient elution, the adsorption isotherm must first be determined at several isocratic points (different fixed φ values).

The Langmuir isotherm model in the isocratic elution mode was considered for further investigation.

$$q=\frac{aC}{1+bC} \tag{8}$$

where b is the equilibrium constant in the overloading condition, $a=q_s b$ is the Henry constant, and q_s is the saturated capacity. In addition, the relationship between k and a is defined as:

$$k=aF \tag{9}$$

where F is defined as the phase ratio ($F=\frac{(1-\varepsilon)(1-\varepsilon_p)}{\varepsilon+(1-\varepsilon)\varepsilon_p}$) [34].

Using Eqs. (7) and (9), the Langmuir isotherm parameters can be

calculated in the gradient elution;

$$a = a_0 e^{-S(\varphi)} \tag{10}$$

$$b = b_0 e^{-S(\varphi)} \tag{11}$$

where $a_0$and b_0 are the adsorption parameters extrapolated at $\varphi = 0$. It must be noted that as a narrow range of φ in the isotherm equation was studied under the gradient elution, q_s is almost considered to be constant. Therefore, by replacing a and b from Eqs (10) and (11) into Eq (8), the Langmuir isotherm model can be obtained for the gradient elution mode;

$$q(c,\varphi) = \frac{q_s b_0 e^{-s(\varphi)} C}{1 + q_s b_0 e^{-s(\varphi)} C} \tag{12}$$

This gradient-adapted Langmuir isotherm was then incorporated into the General Rate Model (GRM) to simulate the elution profiles accurately under overloaded gradient conditions. It is necessary to define both boundary and initial conditions. Danckwerts-type boundary conditions have been employed [29], and the inlet feed gradient has been modeled as follows:

$$\varphi(t,0) = \begin{cases} \varphi_0 & 0 \le t \le t_{inj} \\ \varphi + \dfrac{\Delta\varphi}{t_g}\left(t - t_{inj}\right) & t_{inj} \le t \le t_{inj} + t_g \\ \varphi + \Delta\varphi & t \ge t_{inj} + t_g \end{cases} \tag{13}$$

where t_{inj} is the length of the rectangular injection profile, φ_0 is the initial fraction of the organic modifier and t_g is the time of the gradient.

3. Materials and methods

3.1. Columns and materials

The HPLC-grade acetonitrile (ACN) was purchased from DAEJUNG Chemicals and Metals Co. (Siheung, Korea). HPLC-grade water was obtained from a Millipore Milli-Q purification system (Molsheim, France). Ethanol (99%) was sourced from Kimia Alcohol Zanjan Co. (Zanjan, Iran), and trifluoroacetic acid (TFA) was purchased from Sigma-Aldrich (Darmstadt, Germany). Uracil and Blue dextran 2000 (molecular weight: 2000 kDa) were also purchased from Sigma-Aldrich (Darmstadt, Germany).

For the enrichment step, a macroporous CM2100 resin (Polystyrene-divinylbenzene, PSDVB) obtained from Sun-resin New Materials Co. (Xi'an, Shaanxi, China) with a particle size of 100 μm, was used as the stationary phase. It was packed into stainless steel columns: 250 × 4.6 mm for analytical scale and 250 × 20 mm for preparative scale. For the purification step, commercially available C18 columns from KNAUER (Berlin, Germany) were employed: a 5 μm particle size column (250 × 4.6 mm) for analytical optimization and a 10 μm particle size column (250 × 16 mm) for preparative scale.

Dried *Carthamus tinctorius* L (safflower) plant material was provided from the licensed herbarium of medicinal plants and drugs research institute (SBU, Tehran, Iran). To obtain a safflower extract, 50 g of powdered plant material was mixed with 500 mL of distilled water. The mixture was sonicated for 30 min at room temperature. This extraction procedure was repeated three times to attain the maximum possible yield. Following sonication, the solution was filtered to remove solid residues, and the aqueous extract was concentrated by evaporating the solvent using a rotary evaporator.

3.2. Instrumentation and methods

All analytical and preparative enrichment and purification processes were performed using a KNAUER HPLC system (Berlin, Germany), equipped with a photodiode array PDA detector (Smartline 2800 model), and a binary pump (Smartline pump S1000). The pump included two interchangeable heads with flow capacities of 10 mL/min for the analytical scale and 500 mL/min for the preparative scale.

For HSYA enrichment from the safflower extract, mobile phase A consisted of water with 0.02% TFA, and mobile phase B was 99% ethanol. The column was equilibrated with 10% of mobile phase B for 5 min, followed by a linear gradient to 50% B over 30 min. The gradient was then increased to 100% B over 5 min, and the column was regenerated with 100% B for an additional 5 min. For purification, mobile phase A was water with 0.02% TFA, and mobile phase B was ACN. The column was equilibrated with 10% of mobile phase B for 5 min, followed by a linear gradient to 45% B over 30 min. The gradient was then increased to 100% B over 5 min, and the column was regenerated with 100% B for 5 min. All gradients were performed at a constant flow rate appropriate to the column scale (1 mL/min for analytical and adjusted proportionally for preparative, based on column dimensions).

Fractions collected during enrichment and purification were analyzed off-line using HPLC on a C18 column (5 μm particle size, 250 × 4.6 mm). The mobile phase gradient was the same as for the purification step. Detection was performed using a PDA detector at wavelength of 403 nm relevant to HSYA.

3.2.1. Method for estimating the isotherm parameters

To obtain the adsorption isotherm parameters, overloaded elution profiles were recorded by injecting an HSYA solution at a concentration of 8 g/L. The adsorption isotherm parameters under isocratic elution selected points were calculated using the inverse method [25,44]. By solving the mass balance equations, simulated elution profiles were generated and compared with the experimental profiles. Then, the isotherm parameters were iteratively changed to minimize the difference between the actual and predicted data by minimizing the sum of the squared error technique.

3.2.2. Determination of column porosity, void fraction, and solid porosity

Determination of column porosity, void fraction, and solid porosity is important in modeling the profile peak shapes and locations [28,34]. To calculate the total porosity (ε_t), the uracil as a tracer was injected to determine the dead volume of the column (V_0), including pore volume of solid (V_p).) and interstitial volume (V_{int}). Then, according to Eq. (14), ε_t was obtained by dividing the V_0 to column volume (V_0). However, to attain the void fraction (ε) using Eq. (15), the blue dextran was utilized to determine the interstitial volume exclusively. Ultimately, the solid porosity (ε_p) was calculated using Eq. (16).

$$\varepsilon_t = \frac{V_0}{V_c} \tag{14}$$

$$\varepsilon = \frac{V_{int}}{V_c} \tag{15}$$

$$\varepsilon_p = \frac{\varepsilon_t - \varepsilon}{1 - \varepsilon} \tag{16}$$

4. Results and discussion

4.1. Extraction, enrichment, and purification of HYSA

In this study, a three-step process—extraction, enrichment, and purification—was implemented to achieve the desirable purity. During the extraction, the yellow pigment was extracted from the safflower (*Carthamus tinctorius*) using the ultrasound-assisted method, with water serving as the solvent [45]. The purity at this stage was determined to be 20% by comparing the peak area of HSYA with the total peak area (Fig. 1A). After the extraction step, an enrichment process was performed to remove major impurities. Macroporous resin chromatography was utilized to separate residual impurities from the target compound at both analytical and preparative scales. Macroporous resins, such as the

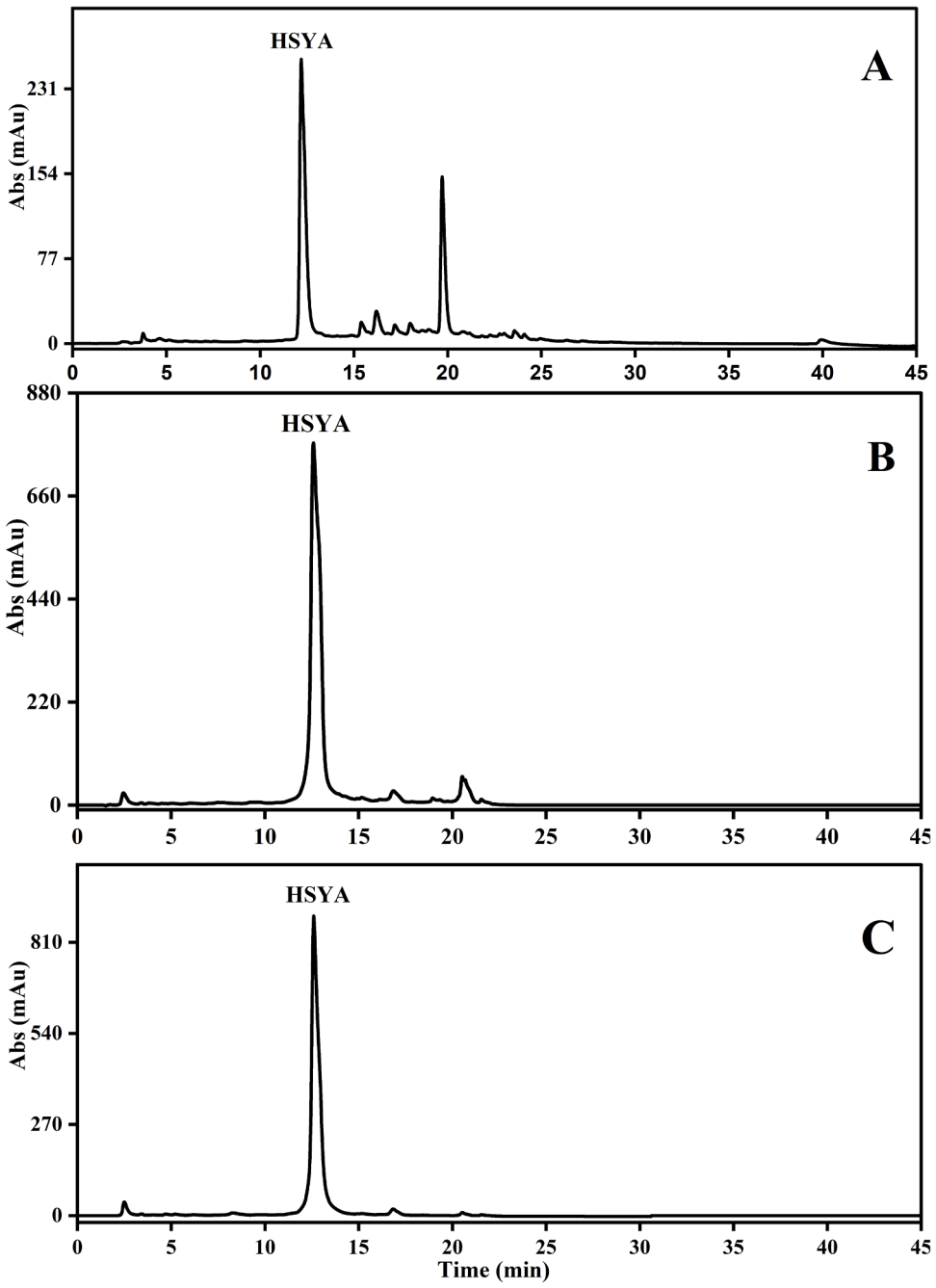

Fig. 1. HPLC-DAD chromatograms recorded at 403 nm. (A) crude extract; (B) enriched extract; (C) purified. d_c: 4.6 mm; L_c: 250 mm.

polystyrene-divinylbenzene (PSDVB)-based CM2100 resin employed in this study, play a pivotal role in this separation due to their distinctive structural characteristics, including large pore diameters (typically 50–1000 nm), high specific surface area, and a hydrophobic polystyrene-divinylbenzene matrix [46]. These features facilitate efficient adsorption of polar yet moderately hydrophobic molecules, such as HSYA. It also provides high loading capacity even under overloaded conditions along with superior selectivity when coupled with gradient elution.

A mathematical model using GRM was developed to evaluate key operating parameters, including loading concentration, injection volume, and column dimensions, as well as to optimize the adsorption isotherm parameters in the analytical scale. The optimized parameters were subsequently scaled up to the preparative level and validated against experimental data.

In the first step of modeling in the enrichment process, estimation of the adsorption isotherm parameters is essential to accurately predict the elution profiles. In this regard, estimating the isotherm parameters under gradient elution conditions is a key objective. To determine the most suitable range of HSYA elution in gradient condition, an overloaded test at a specified concentration was conducted. Fig. 2 presents an experimental chromatogram obtained by injecting certain amount of HSYA solution (50 μL) with an arbitrary overloading concentration of (8 g/L) under the gradient elution conditions in the analytical scale. As can be observed from Fig. 2, the main peak in the chromatogram was eluted at a retention time of approximately 22 min. By considering the dwell volume of the system, this retention time corresponds to a mobile phase composition of about 32.5% ethanol (used as the organic modifier). Therefore, isocratic data were selected in the narrow range of 28–34% ethanol, close to the critical composition where HSYA elutes during the

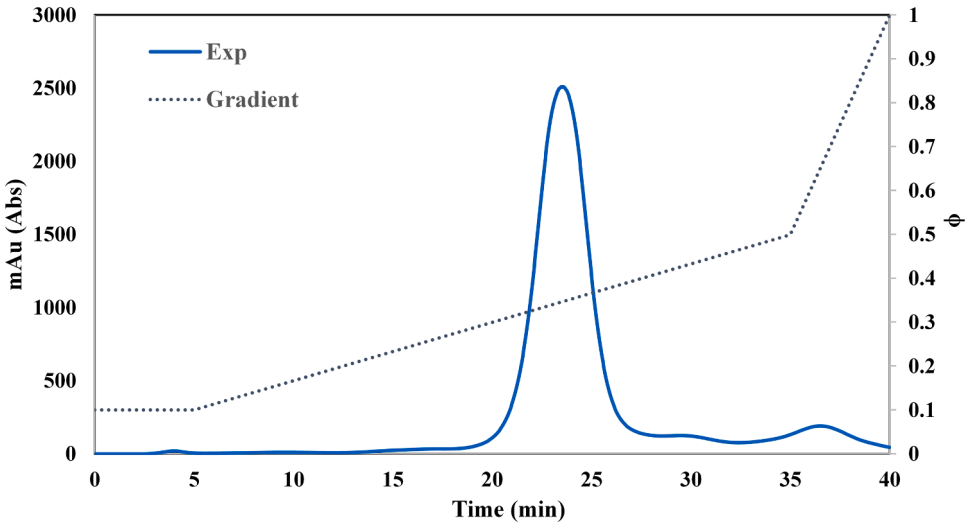

Fig. 2. Experimental gradient elution profile of HSYA solution. Injected concentration: 8 g/L; Injection volume: 50 μL; Wavelength: 403 nm.

gradient run.

The sensitivity of the selected isocratic points on the retention behavior of HSYA was investigated under an infinite dilution of HSYA (0.2 g/L, 50 μL) as shown in **Fig. S1**. As the ethanol percentage increases from 28% to 34%, the retention factor for HSYA changes from 1.63 to 0.64. To better find the retention behavior of HSYA, the stoichiometric displacement model (SDM) has been employed [43,47]. According to this model, the retention behavior is influenced by the displacement of adsorbed molecules on the hydrophobic stationary phase by solvent molecules. It helps to estimate how many solvent molecules are required to replace a single adsorbed analyte molecule, thereby predicting retention trends as a function of solvent strength [48].

$$logk = logI + Z \times log\left(\frac{1}{D_0}\right)$$

In this analysis, k represents the retention factor, D_0 denotes the concentration of organic modifier (ethanol), Z refers to the number of solvent molecules displaced, and I is the extrapolated value of k when $D_0 = 0$ (i.e., in pure water). **Fig S2** illustrates the relationship between log k and log $(\frac{1}{D_0})$ for HSYA. According to the displacement model, the slope of this curve corresponds to Z, and the number of displaced molecules has been estimated. For HSYA, this value was determined to be

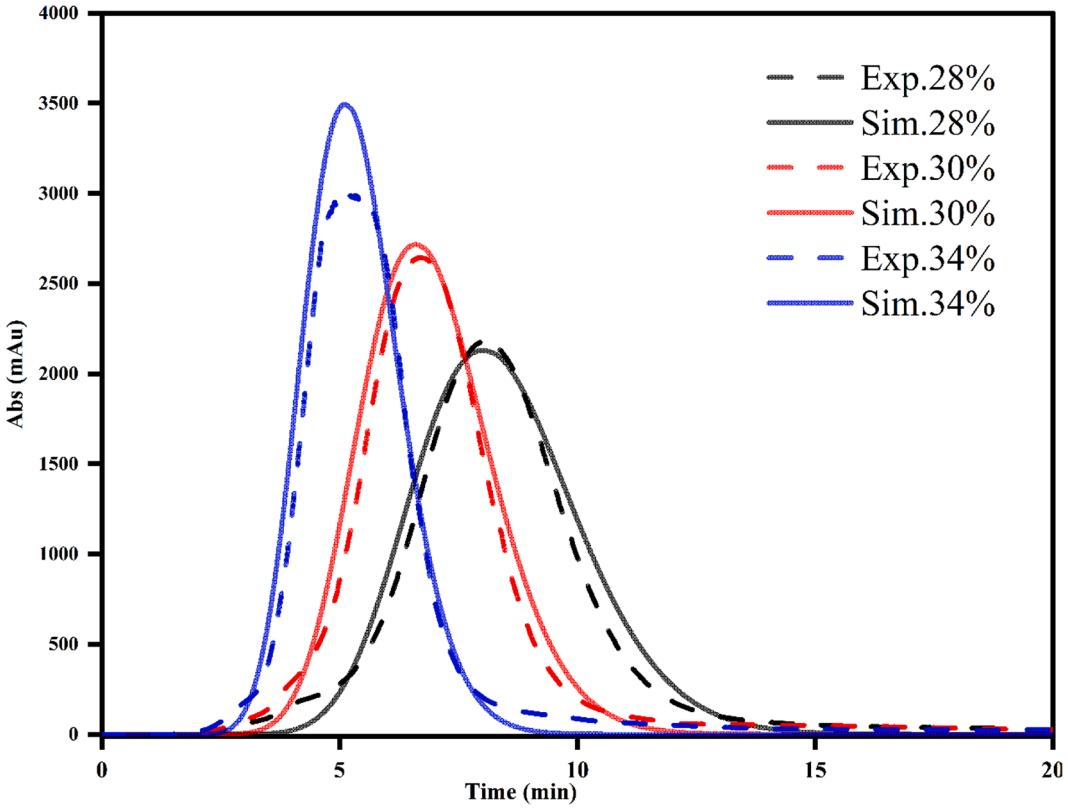

Fig. 3. Comparison between the simulated and experimental elution profiles under the isocratic elution. φ = 28, 30 and 34%; Concentration of HSYA: 8 g/L; Injection volume: 50 μL; Wavelength: 403 nm.

approximately 4.9 ± 0.3. It was revealed that the slope is relatively lower as compared with other reports [49,50], in which the large molecules such as peptides and proteins had been used, rather than the small molecules studied in the present work. However, considering the slope of the curve, it was found that the selected range of the organic modifier was suitable enough for calculating the adsorption isotherm parameters in the isocratic elution conditions.

The inverse method was then applied to determine the isotherm parameters for HSYA.Several adsorption models, including Langmuir, Freundlich, and Freundlich-Langmuir, were evaluated under the isocratic elution on the macroporous resin. Among these, the Langmuir model provided an acceptable fit to experimental elution profiles. As illustrated in Fig. 3 for three selected isocratic points, 28%, 30% and 34% (other isocratic points are presented in the **Fig S3**), there was excellent agreement between the experimental and simulated elution profiles obtained using the GRM for precise prediction in macroporous resin with limited mass transfer. From Fig. 3, the simulated elution profiles exhibited slightly higher peak heights compared with the experimental data, likely due to detector saturation effects observed in the experimental setup, as it was reported in the reference [51].

To further validate the isotherm model, additional overloaded experiments were performed under the isocratic conditions for HSYA concentrations of 8, 16, and 24 g/L in 28% of organic modifier. A constant injection volume of 50 μL was used for all runs. As shown in **Fig. S4** the simulated elution profiles obtained by the GRM were closely matched with the experimental data, confirming that the Langmuir isotherm model adequately describes the adsorption behavior of HSYA on the CM2100 resin under the investigated conditions. It is noteworthy that the high accuracy prediction can be attributed to the ability of GRM to model the axial dispersion which can influence the band broadening particularly in large and different particle sizes distribution associated with macroporous resins [28]. Moreover, relatively low strength elution and surface mobility of the ethanol as an organic modifier limits the rate of mass transfer between the mobile phase and stationary phase that affect the band broadening of the target molecule [52]. The GRM considers the possible effects related to this source of mass transfer limitation on the band broadening. Notwithstanding the aforementioned limitations, the equilibrium isotherm is more important than other phenomena associated with the accurate prediction of elution profiles [29].

Table 2 presents the best isotherm parameters obtained for different organic modifier percentages. As it was aforementioned, according to Eq. (11), by fitting the experimental data (Fig. 4), the amounts of 34 and 2062 L/g for S and b_0 respectively, were obtained for the gradient elution mode. In addition, in the gradient mode, the saturation capacity (q_s) was determined by averaging the values obtained under the isocratic conditions, because the saturation capacities obtained under isocratic conditions showed no significant differences. The average value of 18 g/L was considered for the simulation of gradient elution. These values are substituted in Eq. (12) to model the elution gradient condition using GRM and boundary conditions.

Based on the parameters obtained by fitting the data in Fig. 4 and using the GRM, the elution profiles under the gradient conditions were simulated. Fig. 5 depicts the elution profile of the gradient run of HSYA solutions at concentrations of 8, 16, and 24 g/L. The simulated elution profiles showed acceptable agreement with the experimental results, confirming the reliability of the model. This agreement validated the effectiveness of the selected narrow isocratic range (28–34% ethanol) for accurate estimation of isotherm parameters that can be extrapolated to gradient elution conditions. In detail, as can be seen from Fig. 5, there is a good agreement between the experimental and predicted elution profiles in terms of band widths and retention time, while the peak intensities at concentrations of 16 and 24 g/L were slightly higher than those recorded experimentally (Root mean square error (RMSE) < 4% for retention time, and RMSE < 8% for band width). This discrepancy is primarily attributed to the detector saturation or overloading effects encountered during the actual runs, which likely led to signal compression and underrepresentation of peak intensities in the chromatograms [51]. Overall, these results demonstrated the strength of the GRM in capturing nonlinear adsorption isotherms and mass-transfer phenomena in macroporous resins under gradient elution, particularly for polar natural compounds such as HSYA. The successful prediction of overloaded behavior further highlights the suitability of macroporous resin chromatography combined with rigorous mechanistic modeling for efficient enrichment processes.

Table 2
Adsorption isotherm parameters attained through the inverse method with a Langmuir model at different mobile phase compositions.

φ	a	b (L/g)	q_s (g/L)
0.28	5.20	0.250	21.0
0.29	5.02	0.210	24.0
0.30	3.90	0.185	21.0
0.31	3.30	0.165	20.0
0.32	3.10	0.150	20.6
0.33	2.65	0.140	19.0
0.34	2.23	0.135	16.0

To evaluate the predictive capability of the validated model, the scale-up to the preparative chromatographic column was simulated using the GRM and directly compared with the experimental data. Importantly, the macroporous resin stationary phase, linear velocity, and gradient-adapted isotherm parameters were kept identical according to the analytical scale, ensuring a rigorous and mechanistic scale-up approach. The preparative column dimensions were 250 × 20 mm, with an injection volume of 1000 μL (20-fold increase relative to the analytical scale). The loaded crude extract had a concentration of 100 g/L (corresponding to 100 mg safflower extract containing 20 mg HSYA). The flow rate was scaled to 18 mL/min (18-fold increase) to maintain constant linear velocity. All the other related data have been calculated in **Table S1** and reproducibility of the chromatographic process is reported in **Fig. S5**.

Fig. 6 compares the simulated and experimental elution profiles obtained in the preparative scale. Excellent agreement was observed between the GRM predictions and experimental results in terms of band width, retention time, and peak shape/intensity (RSME < 6%). Minor deviations in tailing could be attributed to the negligible extra-column effects occurring at the higher flow rate. This close match between simulated and experimental elution profiles confirms the robustness and scalability of the GRM when applied to macroporous resin chromatography under overloaded gradient conditions. The successful direct transfer of analytically determined isotherm and mass-transfer parameters to the preparative scale, without any refitting, underscores the power of mechanistic modeling for optimizing the operating conditions and, reliably predicting elution profiles during scale-up of HSYA enrichment processes. Moreover, the presence of impurities in the crude extract have not affected the position of product peak in the simulation result.

The main fraction containing HSYA from the optimized enrichment step was further analyzed by off-line high-performance liquid chromatography (HPLC) (Fig. 1B). It was observed an increase in purity from 20% in the crude extract up to 80% after enrichment (+300%). It must be noted that the overall yield ($\frac{mass\ of\ collected\ fraction}{mas\ of\ product\ in\ the\ injected\ sample}$) in this stage was almost 74% of the product.

In the final purification step, a C18 column was employed. In this stage, initially, the method of elution was optimized systematically to obtain considerable separation between HSYA and other impurities in the analytical scale, and then the elution method was transferred to the preparative column (250 × 16 mm, 10 μm) by preserving the linear velocity and the type of stationary phase. It must be noted that the flow rate in the preparative scale was calculated to be 6 mL.min^{-1} based on Eq. 17. Accordingly, 1 mL of solution with a concentration of 20 g/L of enriched extract was loaded into the preparative column. The main peak that includes HSYA was collected and analyzed by off-line analytical

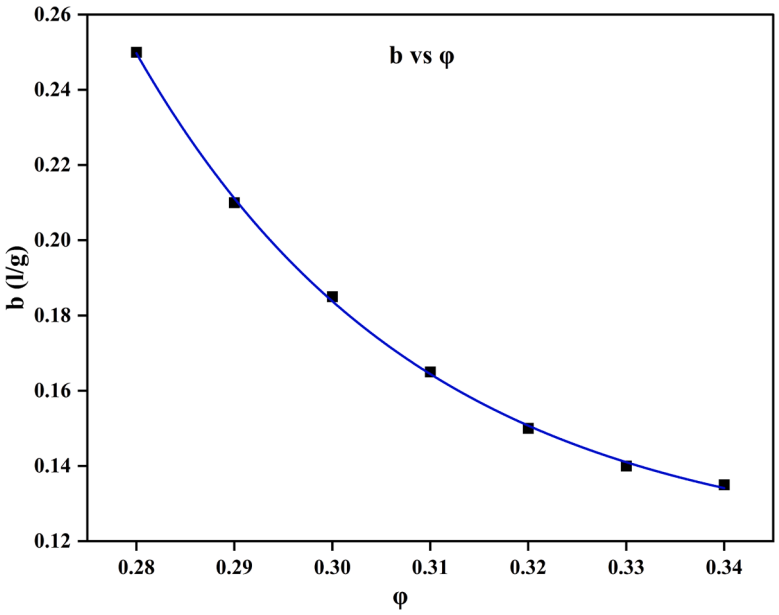

Fig. 4. Relation between the equilibrium adsorption constant (b) and the percentage of organic modifier (φ), $R^2 = 0.99$.

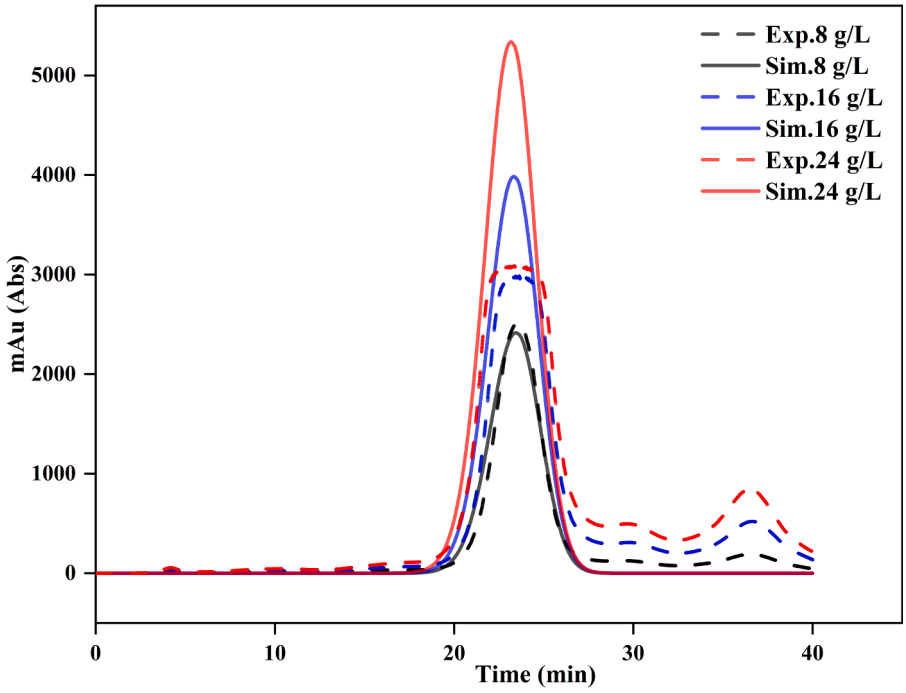

Fig. 5. Comparison of experimental and predicted elution profiles in gradient elution mode. Injection volume: 50 µl; Concentrations of HSYA: 8,16, and 24 g/L; Wavelength: 403 nm.

HPLC (Fig. 1C), showing a further increase in purity up to 95% (+375%).

$$\frac{F_{Prep}}{F_{ana}} = \frac{L_{Prep}}{L_{ana}} \left(\frac{r_{Prep}}{r_{ana}}\right)^2 \frac{D_{ana}}{D_{Prep}} \tag{17}$$

Where, L, r and D are flow rate, length, radius and particle size of analytical and preparative columns, respectively.

5. Conclusion

In this work, the enrichment and purification process of HSYA from safflower extract has been firstly modeled in analytical scale using the inverse method, by investigating retention behavior, phase equilibria and loading conditions. Then the simulation results have been directly used to perform the scale-up to the preparative conditions, by maintaining the type of stationary phase, linear velocity, and isotherm parameters, allowing to reach 95% of final product purity starting from 20%, with an increase of +375%.

This proof-of-concept study further demonstrated that chromatographic modeling can be a useful strategy to transfer purification and isolation process from the analytical scale to the preparative one, without the need for time- and resource-consuming trial-and-error methods, contributing to the green transition of process development.

It is important to point out that this approach can be applied and

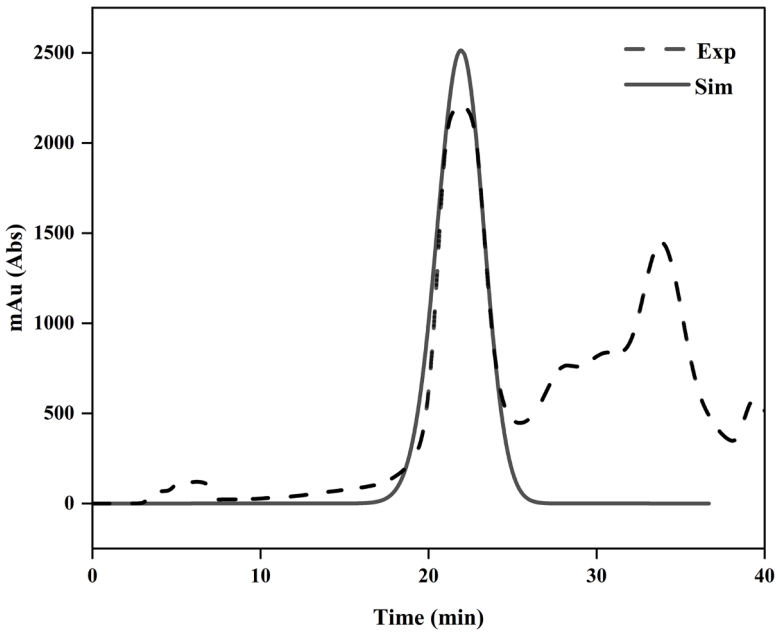

Fig. 6. Comparison between experimental and simulation elution profiles in the preparative scale. Concentration of crude extract: 100 g/L; Injection volume: 1000 μL, Flow rate: 18 mL/min, Wavelength: 403 nm.

extended to other relevant cases, by evaluating and updating isotherm parameters based on the target molecule, chromatographic system and experimental conditions.

CRediT authorship contribution statement

Amin Tabesh: Writing – original draft, Visualization, Validation, Software, Methodology, Formal analysis. **Hassan Rezadoost:** Writing – review & editing, Supervision, Project administration, Data curation, Conceptualization. **Masoud Rahimi:** Writing – review & editing, Validation, Supervision, Data curation. **Hamid Reza Norouzi:** Writing – review & editing, Validation, Supervision, Data curation. **Simona Felletti:** Writing – review & editing, Supervision. **Alberto Cavazzini:** Writing – review & editing.

Declaration of competing interest

The authors declare that they have no known competing financial interests or personal relationships that could have appeared to influence the work reported in this paper.

Acknowledgements

The authors thank the Research Council of the University of Shahid Beheshti University for supporting this work.

The authors would like to thank the National Recovery and Resilience Plan (NRRP), Mission 04 Component 2 Investment 1.5 -NextGenerationEU, Call for tender n. 3277 dated 30/12/2021; Award Number: 0001052 dated 23/06/2022. The authors would also like to thank the Italian University and Scientific Research Ministry (grant P2022PTYWP, title: "Design of highpRofit fostEring bioActive coMpounds through integral valorization of seaWEEDs infesting the MEditerranean sea (DreamWEEDme)" and grant P2022AJA7H8, title "High revenue-generating molecules from industrial hemp: cost-effective, chemical classification-driven solutions for their production (CHempion)" as well as the Regional Programme of the European Regional Development Fund (PR FESR 2021-2027 Priority 1) project title "Production of high-added-value ingredients from fruit supply chain by-products through a cascade biorefinery approach - Frurefinery" for financial support.

Supplementary materials

Supplementary material associated with this article can be found, in the online version, at doi:10.1016/j.chroma.2026.467072.

Data availability

Data will be made available on request.

References

[1] Z. Ekin, Resurgence of safflower (Carthamus tinctorius L.) utilization: a global view, J. Agron. 4 (2005) 83–87.
[2] L. Fan, H.Y. Zhao, M. Xu, L. Zhou, H. Guo, J. Han, B.R. Wang, D.A. Guo, Qualitative evaluation and quantitative determination of 10 major active components in Carthamus tinctorius L. by high-performance liquid chromatography coupled with diode array detector, J. Chromatogr. A. 1216 (2009) 2063–2070, https://doi.org/10.1016/j.chroma.2008.03.046.
[3] I. Adamska, P. Biernacka, Bioactive substances in safflower flowers and their applicability in medicine and health-promoting foods, Int. J. Food Sci. 2021 (2021) 1–23, https://doi.org/10.1155/2021/6657639.
[4] S. Yin, K. Liu, J. Lee, J. Yang, G. Qian, Y. Si, Y. Park, Effect of hydroxysafflor yellow a on tyrosinase: integration of inhibition kinetics with computational simulation, Process. Biochem. 50 (2015) 2112–2120, https://doi.org/10.1016/j.procbio.2015.09.020.
[5] X. Zhang, D. Shen, Y. Feng, Y. Li, H. Liao, Pharmacological actions, molecular mechanisms, pharmacokinetic progressions, and clinical applications of hydroxysafflor yellow a in antidiabetic research, J. Immunol. Res. 2021 (2021) 1–10, https://doi.org/10.1155/2021/4560012.
[6] M. Luo, J. Huang, Z. Yang, Y. Wang, B. Guo, Z. Yue, Hydroxysafflor yellow a exerts beneficial effects via restoring hormone secretion and alleviating oxidative stress in polycystic ovary syndrome mice, Experim. Physiol. 105 (2020) 282–292, https://doi.org/10.1113/EP088147.
[7] T. Bacchetti, C. Morresi, L. Bellachioma, G. Ferretti, Antioxidant and pro-oxidant properties of carthamus tinctorius, hydroxy safflor yellow a, and safflor yellow a, antioxidants. 9 (2020) 119. https://doi.org/10.3390/antiox9020119.
[8] W. Si, W. Yang, D. Guo, J. Wu, J. Zhang, S. Qiu, C. Yao, Y. Cui, W. Wu, Selective ion monitoring of quinochalcone C-glycoside markers for the simultaneous identification of Carthamus tinctorius L. in eleven Chinese patent medicines by UHPLC/QTOF MS, J. Pharm. Biomed. Anal. 117 (2016) 510–521, https://doi.org/10.1016/j.jpba.2015.09.025.
[9] Y. Zhang, L. Yu, W. Jin, C. Li, Y. Wang, H. Wan, J. Yang, Simultaneous optimization of the ultrasonic extraction method and determination of the antioxidant activities of hydroxysafflor yellow A and anhydrosafflor yellow B from safflower using a response surface methodology, Molecules 25 (2020) 1226, https://doi.org/10.3390/molecules25051226.

[10] A. Savcenco, Spectral and chromatographic characterisation of the yellow food dye from safflower, J. Eng. Sci. 29 (2022) 189–195, https://doi.org/10.52326/jes.utm.2022.29(3).16.

[11] Z. Yan, R. Alimu, J. Wan, X. Liao, S. Lin, S. Dai, F. Chen, S. Zhang, Y. Tong, H. Liu, R. Qin, J. Liu, Composition of major quinochalcone hydroxysafflor yellow A and anhydrosafflor yellow B is associated with colour of safflower (Carthamus tinctorius) during colour-transition but not with overall antioxidant capacity: a study on 144 cultivars, Food Res. Int. 162 (2022) 112098, https://doi.org/10.1016/j.foodres.2022.112098.

[12] S. Yue, Y. Tang, C. Xu, S. Li, Y. Zhu, J.A. Duan, Two new quinochalcone C-Glycosides from the florets of Carthamus tinctorius, Int. J. Mol. Sci. 15 (2014) 16760–16771, https://doi.org/10.3390/ijms150916760.

[13] K. Inoue, C. Nomura, Y. Mizuno, Y. Yoshimi, K. Tsutsumiuchi, T. Hino, H. Oka, Separation of major safflowers from Carthamus yellow using high-speed countercurrent chromatography, J. Liq. Chromatogr. Relat. Technol. 31 (2008) 1047–1059, https://doi.org/10.1080/10826070801925011.

[14] C. Qu, L.Y. Wang, W.T. Jin, Y.P. Tang, Y. Jin, X.Q. Shi, L.L. Shang, E.X. Shang, J. A. Duan, Comparative analysis of the effects of hydroxysafflor yellow A and anhydrosafflor yellow B in safflower series of herb pairs using prep-HPLC and a selective knock-out approach, Molecules 21 (2016) 1480, https://doi.org/10.3390/molecules21111480.

[15] C.K.S. Ng, H. Osuna-Sanchez, E. Valéry, E. Sørensen, D.G. Bracewell, Design of high productivity antibody capture by protein A chromatography using an integrated experimental and modeling approach, J. Chromatogr. B Anal. Technol. Biomed. Life Sci. 899 (2012) 116–126, https://doi.org/10.1016/j.jchromb.2012.05.010.

[16] T. Svoboda, S. Henke, S. Gillarová, M. Sluková, M. Isoz, C. Hamel, Model-based scaling of preparative chromatographic separation of sucrose and glucose using bilevel parameter estimation for equilibrium dispersive model with nonlinear isotherm, J. Chromatogr. A. 1757 (2025) 466135, https://doi.org/10.1016/j.chroma.2025.466135.

[17] S. Qamar, N. Rehman, G. Carta, A. Seidel-morgenstern, Analysis of gradient elution chromatography using the transport model, Chem. Eng. Sci. 225 (2020) 115809, https://doi.org/10.1016/j.ces.2020.115809.

[18] J. Weon, A. Kienle, A. Seidel-morgenstern, On-line optimization of four-zone simulated moving bed chromatography using an equilibrium-dispersion model: II. Experimental validation, Chem. Eng. Sci. 226 (2020) 115808, https://doi.org/10.1016/j.ces.2020.115808.

[19] H. Narayanan, T. Seidler, M.F. Luna, M. Sokolov, M. Morbidelli, A. Butté, Hybrid Models for the simulation and prediction of chromatographic processes for protein capture, J. Chromatogr. A. 1650 (2021) 462248, https://doi.org/10.1016/j.chroma.2021.462248.

[20] G. Sodeifian, S.A. Sajadian, N. Saadati Ardestani, Experimental optimization and mathematical modeling of the supercritical fluid extraction of essential oil from Eryngium billardieri: application of simulated annealing (SA) algorithm, J. Supercrit. Fluids. 127 (2017) 146–157, https://doi.org/10.1016/j.supflu.2017.04.007.

[21] W. Jones, D.I. Gerogiorgis, A model-based performance analysis of integrated chromatography-ultrafilter separation systems for monoclonal antibody (mAb) manufacturing, Biochem. Eng. J. 206 (2024) 109281, https://doi.org/10.1016/j.bej.2024.109281.

[22] M. Hooshyari, H. Rezadoost, H. Reza, Sequential purification of cannabidiol by two-dimensional liquid chromatography combined with modeling and simulation of elution profiles, J. Chromatogr. A. 1717 (2024) 464702, https://doi.org/10.1016/j.chroma.2024.464702.

[23] L.J. Benedini, D. Figueiredo, J. Cabrera-Crespo, V.M. Gonçalves, G.G. Silva, G. Campani, T.C. Zangirolami, F.F. Furlan, Modeling and simulation of anion exchange chromatography for purification of proteins in complex mixtures, J. Chromatogr. A. 1613 (2020) 460685, https://doi.org/10.1016/j.chroma.2019.460685.

[24] S.M.J. Hossienizadeh, M. Bagheri, M. Alizadeh, M. Rahimi, S.M. Azimi, M. Kamalzade, A. Es-haghi, A. Ghassempour, Two dimensional anion exchange-size exclusion chromatography combined with mathematical modeling for downstream processing of foot and mouth disease vaccine, J. Chromatogr. A. 1643 (2021) 462070, https://doi.org/10.1016/j.chroma.2021.462070.

[25] C. De Luca, S. Felletti, M. Macis, W. Cabri, G. Lievore, T. Chenet, L. Pasti, M. Morbidelli, A. Cavazzini, M. Catani, A. Ricci, Modeling the nonlinear behavior of a bioactive peptide in reversed-phase gradient elution chromatography, J. Chromatogr. A. 1616 (2020) 460789, https://doi.org/10.1016/j.chroma.2019.460789.

[26] A.P. Sabharwal, H.A. Chase, Preparative reversed-phase high performance liquid chromatography of insulin variants: characterization of adsorption isotherms by frontal analysis, Food Bioprod. Process. Trans. Inst. Chem. Eng. Part C. 77 (1999) 18–26, https://doi.org/10.1205/096030899532213.

[27] J. Lindholm, P. Forsse, T. Fornstedt, Validation of the accuracy of the perturbation binary adsorption isotherm parameters in LC, Anal. Chem. 76 (2004) 5472–5478, https://doi.org/10.1021/ac049632k.

[28] H. Schmidt-Traub, M. Schulte, A. Seidel-Morgenstern, Preparative Chromatography, John Wiley & Sons, 2020.

[29] G. Guiochon, A. Felinger, D.G. Shirazi, Fundamentals of Preparative And Nonlinear Chromatography, Elsevier, 2006.

[30] A. Felinger, D. Zhou, G. Guiochon, Determination of the single component and competitive adsorption isotherms of the 1-indanol enantiomers by the inverse method, J. Chromatogr. A. 1005 (2003) 35–49, https://doi.org/10.1016/S0021-9673(03)00889-6.

[31] J. Xu, L. Zhu, G. Xu, W. Yu, A.K. Ray, Determination of competitive adsorption isotherm of enantiomers on preparative chromatographic columns using inverse method, J. Chromatogr. A. 1273 (2013) 49–56, https://doi.org/10.1016/j.chroma.2012.11.052.

[32] A. Felinger, A. Cavazzini, G. Guiochon, Numerical determination of the competitive isotherm of enantiomers, J. Chromatogr. A. 986 (2003) 207–225, https://doi.org/10.1016/S0021-9673(02)01919-2.

[33] K. Kaczmarski, Estimation of adsorption isotherm parameters with inverse method—possible problems, J. Chromatogr. A. 1176 (2007) 57–68, https://doi.org/10.1016/j.chroma.2007.08.005.

[34] T. Gu, Mathematical modeling and scale-up of liquid chromatography: with application examples, second edition, 2015. https://doi.org/10.1007/978-3-319-16145-7.

[35] S. Qamar, J. Nawaz, A. Mehwish, Linear general rate model of chromatography for core – shell particles: analytical solutions and moment analysis, Chem. Eng. Sci. 137 (2015) 352–363, https://doi.org/10.1016/j.ces.2015.06.053.

[36] T. Gu, M. Liu, K.S.C. Cheng, S. Ramaswamy, C. Wang, A general rate model approach for the optimization of the core radius fraction for multicomponent isocratic elution in preparative nonlinear liquid chromatography using cored beads, Chem. Eng. Sci. 66 (2011) 3531–3539, https://doi.org/10.1016/j.ces.2011.04.021.

[37] C.E. Borba, R. Guirardello, E.A. Silva, M.T. Veit, C.R.G. Tavares, Removal of nickel (II) ions from aqueous solution by biosorption in a fixed bed column: experimental and theoretical breakthrough curves, Biochem. Eng. J. 30 (2006) 184–191, https://doi.org/10.1016/j.bej.2006.04.001.

[38] S.O. Rastegar, T. Gu, Empirical correlations for axial dispersion coefficient and Peclet number in fixed-bed columns, J. Chromatogr. A. 1490 (2017) 133–137, https://doi.org/10.1016/j.chroma.2017.02.026.

[39] E.J. Wilson, C.J. Geankoplis, Liquid mass transfer at very low Reynolds numbers in packed beds, Ind. Eng. Chem. Fundam. 5 (1966) 9–14.

[40] D. Antos, W. Piątkowski, K. Kaczmarski, Determination of mobile phase effect on single-component adsorption isotherm by use of numerical estimation, J. Chromatogr. A. 874 (2000) 1–12, https://doi.org/10.1016/S0021-9673(00)00082-0.

[41] C.F. Poole, S.N. Atapattu, Analysis of the solvent strength parameter (linear solvent strength model) for isocratic separations in reversed-phase liquid chromatography, J. Chromatogr. A. 1675 (2022) 463153, https://doi.org/10.1016/j.chroma.2022.463153.

[42] T. Takeuchi, L.R. Snyder, J.W. Dolan, High-performance gradient elution. The practical application of the linear-solvent-strength model, Anal. Bioanal. Chem. 389 (2007) 1659–1660, https://doi.org/10.1007/s00216-007-1557-8.

[43] M.R. Euerby, F. Scannapieco, H.J. Rieger, I. Molnar, Retention modelling in ternary solvent-strength gradient elution reversed-phase chromatography using 30 mm columns, J. Chromatogr. A. 1121 (2006) 219–227, https://doi.org/10.1016/j.chroma.2006.04.073.

[44] C. De Luca, G. Compagnin, C. Nosengo, G. Mazzoccanti, F. Gasparrini, A. Cavazzini, M. Catani, S. Felletti, Novel insights into the dependence of adsorption-desorption kinetics on particle geometry in chiral chromatography, Anal. Bioanal. Chem. 416 (2024) 1809–1820, https://doi.org/10.1007/s00216-024-05186-z.

[45] Y. Ji, S. Guo, B. Wang, M. Yu, Extraction and determination of flavonoids in Carthamus tinctorius, Open Chem. 16 (2018) 1129–1133, https://doi.org/10.1515/chem-2018-0119.

[46] Y. Bai, P. Lu, C. Han, C. Yu, M. Chen, F. He, D. Yi, L. Wu, Hydroxysafflor yellow a (HSYA) from flowers of carthamus tinctorius L. and its vasodilatation effects on pulmonary artery, Molecules 17 (2012) 14918–14927, https://doi.org/10.3390/molecules171214918.

[47] L. Pasti, N. Marchetti, R. Guzzinati, M. Catani, V. Bosi, F. Dondi, A. Sepsey, A. Felinger, A. Cavazzini, Microscopic models of liquid chromatography: from ensemble-averaged information to resolution of fundamental viewpoint at single-molecule level, TrAC - Trends Anal. Chem. 81 (2016) 63–68, https://doi.org/10.1016/j.trac.2015.08.007.

[48] F. Wang, F. Yang, Y. Tian, J. Liu, J. Shen, Q. Bai, Studies on the retention mechanism of solutes in hydrophilic interaction chromatography using stoichiometric displacement theory I. The linear relationship of lgk' vs. lg[H2O], Talanta 176 (2018) 499–508, https://doi.org/10.1016/j.talanta.2017.08.062.

[49] E. Tyteca, J. De Vos, N. Vankova, P. Cesla, G. Desmet, S. Eeltink, Applicability of linear and nonlinear retention-time models for reversed-phase liquid chromatography separations of small molecules, peptides, and intact proteins, J. Sep. Sci. 39 (2016) 1249–1257, https://doi.org/10.1002/jssc.201501395.

[50] A. Tabesh, C. De Luca, A. Faraji, R. Canton, M. Catani, A. Cavazzini, H. Rezadoost, C. Nosengo, S. Felletti, Expanding the use of green solvents for the isolation of melittin from honeybee venom, J. Chromatogr. A. 1763 (2025) 466460, https://doi.org/10.1016/j.chroma.2025.466460.

[51] G. Compagnin, C. De Luca, C. Nosengo, M. Catani, A. Cavazzini, G. Greco, Y. Krauke, S. Felletti, Sustainable cannabinoids purification through twin-column recycling chromatography and green solvents, Anal. Bioanal. Chem. 416 (2024) 4091–4099, https://doi.org/10.1007/s00216-024-05332-7.

[52] D. Bozza, C. De Luca, S. Felletti, M. Spedicato, F. Presini, P.P. Giovannini, M. Carraro, M. Macis, A. Cavazzini, M. Catani, A. Ricci, W. Cabri, Dimethyl carbonate as a green alternative to acetonitrile in reversed-phase liquid chromatography. Part II: purification of a therapeutic peptide, J. Chromatogr. A. 1713 (2024) 464530, https://doi.org/10.1016/j.chroma.2023.464530.